Uniformity of postprocessing of dense nanotube arrays by neutral and ion fluxes

Cite as: Appl. Phys. Lett. **89**, 223108 (2006); https://doi.org/10.1063/1.2388941
Submitted: 11 September 2006 . Accepted: 05 October 2006 . Published Online: 28 November 2006

I. Levchenko, K. Ostrikov, and E. Tam

Uniformity of postprocessing of dense nanotube arrays by neutral and ion fluxes

I. Levchenko, K. Ostrikov,[a] and E. Tam
Plasma Nanoscience@Complex Systems, School of Physics, The University of Sydney, Sydney, New South Wales 2006, Australia

(Received 11 September 2006; accepted 5 October 2006; published online 28 November 2006)

The advantages of using low-temperature plasma environments for postprocessing of dense nanotube arrays are shown by means of multiscale hybrid numerical simulations. By controlling plasma-extracted ion fluxes and varying the plasma and sheath parameters, one can selectively coat, dope, or functionalize different areas on nanotube surfaces. Conditions of uniform deposition of ion fluxes over the entire nanotube surfaces are obtained for different array densities. The plasma route enables a uniform processing of lateral nanotube surfaces in very dense (with a step-to-height ratio of 1:4) arrays, impossible via the neutral gas process wherein radical penetration into the internanotube gaps is poor. © *2006 American Institute of Physics*. [DOI: 10.1063/1.2388941]

Compact arrays of vertically aligned carbon nanotubes[1] (CNTs) such as CNT forests[2] and bundles[3] hold an outstanding promise for various applications owing to the many unique properties of the CNTs.[4] Such arrays find numerous applications in electron field emitters,[5] chemical sensors,[6] high-frequency transistors,[7] reinforcement materials,[8] nanoelectronic devices,[9] nanoswitches,[10] and several others. Recent research suggests that postprocessing (e.g., coating, doping, or functionalization) of nanotube surfaces can significantly improve several structural, electronic, mechanical, and other CNT properties and dramatically expand the field of CNT applications. This opens broad avenues for the use of CNTs in various advanced devices that require controlled electric capacitance,[11] thermal resistivity,[12] hydrophobic properties,[3] or interconnection between different nanotubes in nanoelectronics.[13] Relevant examples include coating of CNT surfaces by amorphous SiO_2 (Ref. 14) for better integration in silicon-based ultralarge scale integrated microelectronic technology, deposition of nonwetting polymer layers for biodevice applications, or tungsten disulfide films for the development of new-generation light-emitting devices.[15] Meanwhile, functionalization of nanotube surfaces is commonly achieved, e.g., by using neutral fluxes of atomic hydrogen,[16] organic molecules,[17] or fluorine-based species.[18]

Despite a remarkable recent progress in postprocessing of individual CNTs and low-density nanotip patterns, a similar treatment of dense nanotube arrays (which result from the most widely used porous template techniques[5]) still remains a major challenge. The main issue is to achieve a high level of control and selectivity in the coating or doping/functionalization of specific surface areas of the nanostructures. For example, few-monolayer-thin films uniformly covering the entire surface of every nanotube in the array are of special interest. However, using liquid reagent solutions for such a purpose often appears problematic (even in the case of relatively low-density patterns) because of significant limitations of the reagent penetration into the internanotube space due to the surface tension forces. The use of the neutral and ionized gas-based processes, commonly adopted for synthesizing CNT arrays, would be a possible alternative. Some of the most popular methods of the CNT fabrication are the chemical vapor deposition (CVD),[19] plasma-enhanced CVD,[20] arc discharges,[21,22] and rf magnetron sputtering.[23] In this regard, plasma-aided methods have several important advantages, such as better vertical alignment and ordering in the pattern,[24] deterministic shape control,[25] and several others.[26] The aim of this Letter is to use numerical simulations to show advantages of the plasma-based postprocessing of dense carbon nanotube arrays, as compared to neutral gas process.

Here we simulate a process of nanotube array coating/treatment in neutral and ionized gas-based environments. We consider a typical array of CNTs of 2 μm in height and 100 nm in diameter as sketched in Fig. 1. The CNTs are arranged in the hexagonal pattern shown in Fig. 1(c), with the spacing Δ between the nanostructures varying from 500 nm (dense forest) to 4 μm (rarefied CNT array) [Figs. 1(a) and 1(b)]. This spacing is usually controlled by prepatterning Ni/Fe/Co catalysts. In the neutral gas flux, the species of mass m_n move with the uniformly space-distributed thermal velocity $(2k_BT_g/m_n)^{1/2}$, where k_B is the Boltzmann constant and T_g is the gas temperature (in Kelvin). In the plasma-based process, the ions are extracted from the plasma bulk and appear at the sheath border with the velocities directed normally to the substrate surface. To be specific, we have considered only neutral Si and single-charged Si^+ silicon species with the atom mass of 28. The potential drop U_B across the near-substrate sheath has been varied from the floating potential to a typical dc substrate bias of −50 V, and the electron temperature T_e was varied from 2 to 5 eV. Thus, we have adopted typical conditions of the synthesis of defect-free, undamaged CNTs in low-temperature plasmas.

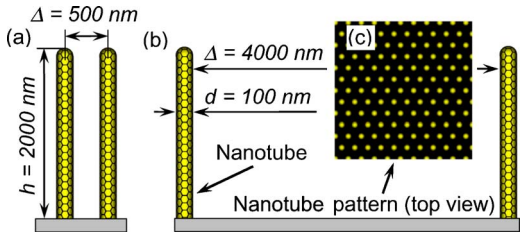

FIG. 1. (Color online) Schematics of dense ($h/\Delta=4$) (a) and rarefied ($h/\Delta=1/2$) (b) nanotube arrays and hexagonal (top view) nanotube pattern used in simulations (c).

[a]Electronic mail: k.ostrikov@physics.usyd.edu.au

The sheath thickness was estimated as $\lambda = \gamma\sqrt{\varepsilon_0 T_e/ne}(2U_B/T_e)^{3/4}$, where γ is a constant typically ranging from 1 to 5,[27] ε_0 is the dielectric constant, n is the plasma density, and e is the electron charge.

The electric potential in the CNT array, $\varphi(r) = \int_S(\rho/4\pi\varepsilon_0 r)dS$, where ρ is the electric charge density on the nanotube surfaces and S is the total simulation area, depends on the nanotube geometry and density on the substrate. In this work our focus is on elongated cylindrical nanotubes with hemispherical caps on top, creating much stronger electric field near the upper parts of the nanotubes. The total electric potential was decomposed into the potential of the flat substrate surface, $\varphi_w = U_B(z/\lambda)^{1/3}$, where z is the normal distance to the surface; potentials of cylindrical lateral surfaces of each (ith) nanotube,

$$\varphi_{c.i}(r) = \frac{\rho}{4\pi\varepsilon_0}\int_0^h \int_0^{2\pi} \frac{r\bar{r}_{0.i}d\alpha d\bar{h}}{\sqrt{\bar{h}_i^2 + \bar{r}_{0.i}^2 + 1 - 2\bar{r}_{0.i}\cos(\alpha)}}, \quad (1)$$

$$\varphi_{S.i}(r) = \frac{\rho}{4\pi\varepsilon_0}\int_0^{\pi/2} \int_0^{2\pi} \frac{r\bar{r}_{0.i}^2 d\alpha d\beta}{\sqrt{\bar{r}_{0.i}^2 - 2\bar{r}_{0.i}\cos(\alpha)\cos(\beta) + 1}}, \quad (2)$$

where $\bar{h}_i = h_i/r$, h_i is the height of the ith nanotube, $\bar{r}_{0,i} = r_{0,i}/r$, and $r_{0,i}$ is the radius of the ith CNT. The total electric potential at the ion position (characterized by the ion position vector $\mathbf{r}_i$),

$$\varphi(r) = \varphi_w + \sum_1^N \varphi_{c.i} + \sum_1^N \varphi_{c.i}, \quad (3)$$

was calculated by summation of the potentials of the substrate surface and all N nanotubes within the array. The electric charge density of the CNT surface was calculated by equating the nanotube electric potential to that of the substrate. The ion dynamics was modeled by integrating the equations of ion motion in the complex electric field described by the electrical potential [Eq. (3)].

The distributions of the atom/ion fluxes over the nanotube surfaces were computed by the Monte Carlo technique, with the total number of the species traced up to 10^5. The results of the atom/ion motion simulations were used to plot the atom and ion flux distributions along the nanotube length. The simulation area in the substrate surface was 25×25 μm. The nanotubes were arranged into the hexagonal pattern [Fig. 1(c)]; the number of the CNTs varied from 200 (rarefied array) to 10^4 (dense array). We limited the study to delicate postprocessing such as deposition of ultrathin (a-few-monolayer) coatings onto CNT surfaces, using the dose changing from 1 to 5 ML, where 1 ML is $\sim 4\times 10^{18}$ m^{-2} for silicon. The net dose actually required to deposit a single monolayer over all nanotube surfaces (excluding the open surface areas) varied from 0.05 ML for a rarefied array ($\Delta = 4$ μm) to 3 ML for a high-density array ($\Delta = 0.5$ μm). The other parameters used in simulations are plasma density $n = 10^{17}$ to 5×10^{18} m^{-3}, gas temperature $T_g = 1000$ K, and gas pressure $p_0 = 1$ Pa.

The numerical experiments have revealed quite different trajectories of the neutral and ionic species in dense nanotube arrays. The atoms were randomly distributed in the velocity space and mainly deposited onto the upper parts of the nanotube surface, showing a shallow penetration into the internanotube gaps [Fig. 2(a)]. On the contrary, the ions were effectively focused by the electric field and drawn deeper into the voids between the CNTs. Afterwards, the ions were deflected by the electric field created by the cylindrical nanotube segments and eventually deposited on their lateral surfaces as shown in Fig. 2(b).

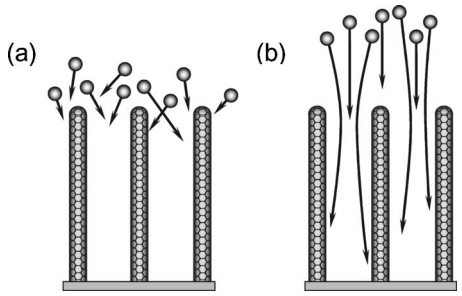

FIG. 2. Neutral (a) and ion fluxes (b) in a dense nanotube array.

Figure 3 shows the neutral atom distribution on the nanotube lateral surface with the internanotube spacing as a parameter. It is seen that the atom penetration into the internanotube gap is more or less satisfactory only for the large enough spacing $\Delta = 2$ μm (i.e., when the spacing is equal to the nanotube height) and significantly decreases when the internanotip gaps become smaller. Remarkably, the nonuniformity of the neutral flux deposition reaches 50% for $\Delta = 1$ μm and even 98% for $\Delta = 500$ nm as can be seen in Fig. 3. Keeping in mind that a CNT array with the spacing ratio $\mu = \Delta/h$ (internanotube spacing to nanotube height) of 0.5 and below is a typical example of a dense nanotube forest, one can conclude that the neutral gas-based coating/functionalization in this case is very nonuniform due to unsatisfactory neutral flux penetration into the internanotube space. In this case, the atoms may reach the lower parts of the CNTs only via migration over the CNT lateral surfaces, a process with a quite limited controllability.[3]

The results of computations made for the ion flux extracted from the plasma under various parameters are shown in Figs. 4(a) and 4(b) for the two different internanotube spacings $\Delta = 500$ nm and $\Delta = 2$ μm, respectively. It is clearly seen that the ion flux distribution over the nanotube lateral surface is quite similar for small and large internanotube gaps. However, the effect of the plasma-surface sheath width appears to be very strong in both cases. Indeed, when the plasma sheath is thin (which is the case for the higher plasma density or electron temperature and/or lower substrate bias), the ion flux is predominantly deposited onto the upper sections of the nanotubes. When the sheath is enlarged (e.g., by decreasing the plasma density or electron temperature and/or increasing the substrate bias), the maximum of the ion flux distribution is shifted towards the substrate surface. In this

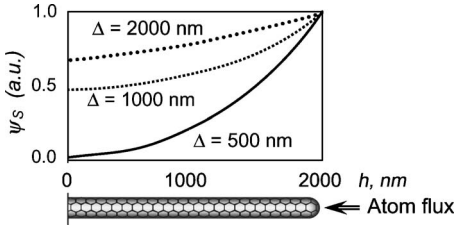

FIG. 3. Normalized distribution of the neutral flux over CNT lateral surfaces with intertube spacing Δ as a parameter.

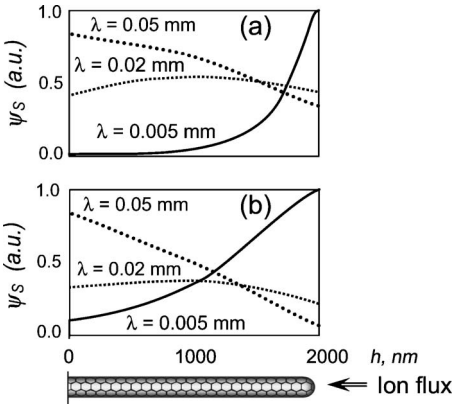

FIG. 4. Normalized distribution of the ion flux over the nanotube lateral surface with the sheath thickness as a parameter. Internanotube spacings $\Delta = 500$ nm (a) and $\Delta = 2$ μm (b).

case the flux covers the entire lateral surface of the nanotubes and becomes very uniform for the sheath of the 0.02 mm width, as can be seen in Fig. 4. A further increase of the sheath width causes more ions to deposit in the areas closer to the substrate surface (bold dotted lines in Fig. 4). When the sheath width increases to $\lambda = 0.05$ mm (e.g., when $T_e = 5$ eV, $n = 2 \times 10^{18}$ m^{-3}, and $U_B = -50$ V), one obtains a trianglelike ion flux distribution with the maximum near the substrate surface.

Thus, the results of our numerical experiments suggest that the use of the plasma-based process leads to a better controllability of the distribution of the "working species" required for postprocessing of dense nanotube arrays. Indeed, in contrast to the neutral gas route, the ion current can be selectively directed to the upper or lower sections of the CNT lateral surfaces, and, if necessary, uniformly not exceeding 20% (short dashed lines in Fig. 4). The uniform ion flux distribution can be obtained even for rather dense nanotube forests with the spacing ratio $\mu = 0.25$.

The possibility of selective coating and functionalization of different parts (e.g., of upper or lower sections of the cylindrical surfaces or caps) of CNTs arranged in dense arrays is undoubtedly very promising for complex postprocessing. For example, ultrathin films of highly emissive materials may be required at the upper parts of the nanotubes to enhance the electron field emission, whereas surface coating by highly conducting materials or introduction of special dopants can be useful to enhance the conductivity of the CNT-based microemitters. Such a complex treatment can be achieved by using a two-stage plasma-based process, wherein the species of a low-work-function material can be directed to the upper sections, followed by the uniform deposition of the ions of a highly conductive material over the lateral CNT surface. This effect can also significantly improve the controllability of the CNT growth process. Indeed, by manipulating the plasma parameters, ionic building units can be selectively delivered to metal catalyst particles located either on the top or at the base of the nanostructures depending on the prevailing CNT growth mode. This can also affect the thermokinetic growth mode selection, which in turn controls the nanotube structure (single or multiwalled, capped or open ended, chirality, etc.). To this end, selective and highly controlled delivery of reactive species from the plasma to specified areas of dense-arrayed CNTs can be instrumental for the deterministic tuning of CNT properties required in the envisaged applications.

In summary, by means of multiscale hybrid numerical simulations, we have shown the advantages of low-temperature plasmas for postprocessing of dense arrays of vertically aligned carbon nanotubes. By using the plasma-extracted ion fluxes, the CNTs can be uniformly coated and treated along the entire length. The uniformity of the ion flux deposition is the best when the thickness of the plasma sheath is approximately one order of magnitude larger than the nanotube length. Manipulating the plasma parameters makes it possible to direct the ion flux to preselected areas on the nanotube surfaces. This effect can also be used for deterministic synthesis of dense CNT arrays in low-temperature plasmas. This work was partially supported by the Australian Research Council, the University of Sydney.

[1] V. P. Veedu, A. Cao, X. Li, K. Ma, C. Soldano, S. Kar, P. M. Ajayan, and M. N. Ghasemi-Nejhad, Nat. Mater. **5**, 457 (2006).
[2] O. A. Louchev, Y. Sato, and H. Kanda, Appl. Phys. Lett. **80**, 2752 (2002).
[3] M. Terrones, N. Grobert, J. Olivares, J. P. Zhang, H. Terrones, K. Kordatos, W. K. Hsu, J. P. Hare, P. D. Townsend, K. Prassides, A. K. Cheetham, H. W. Kroto, and D. R. M. Walton, Nature (London) **388**, 52 (1997).
[4] M. Keidar, Y. Raitses, A. Knapp, and A. M. Waas, Carbon **44**, 1022 (2006).
[5] S.-H. Jeong, H.-Y. Hwang, K.-H. Lee, and Y. Jeong, Appl. Phys. Lett. **78**, 2052 (2001).
[6] K. Bradley, J.-C. P. Gabriel, A. Star, and G. Grüner, Appl. Phys. Lett. **83**, 3821 (2003).
[7] Z. Yu, C. Rutherglen, and P. J. Burke, Appl. Phys. Lett. **88**, 233115 (2006).
[8] J. Zhu, H. Peng, F. Rodriguez-Macias, L. J. Margrave, N. V. Khabashesku, M. A. Imam, K. Lozano, and V. E. Barrera, Adv. Funct. Mater. **14**, 643 (2004).
[9] J. D. Long, S. Xu, S. Y. Huang, P. P. Rutkevych, M. Xu, and C. H. Diong, IEEE Trans. Plasma Sci. **33**, 240 (2005).
[10] E. Dujardin, V. Derycke, M. F. Goffman, R. Lefèvre, and J. P. Bourgoin, Appl. Phys. Lett. **87**, 193107 (2005).
[11] Y.-T. Kim, Y. Ito, K. Tadai, T. Mitani, U.-S. Kim, H.-S. Kim, and B.-W. Cho, Appl. Phys. Lett. **87**, 234106 (2005).
[12] S. Shenogin, A. Bodapati, L. Xue, R. Ozisik, and P. Keblinski, Appl. Phys. Lett. **85**, 2229 (2004).
[13] P. W. Chiu, G. S. Duesberg, U. Dettlaff-Weglikowska, and S. Roth, Appl. Phys. Lett. **80**, 3811 (2002).
[14] E. A. Whitsitt and A. R. Barron, Nano Lett. **3**, 775 (2003).
[15] V. Stolojan, S. R. P. Silva, M. J. Goringe, R. L. D. Whitby, W. K. Hsu, D. R. M. Walton, and H. W. Kroto, Appl. Phys. Lett. **86**, 063112 (2005).
[16] B. N. Khare, M. Meyyappan, J. Kralj, P. Wilhite, M. Sisay, H. Imanaka, J. Koehne, and C. W. Baushchlicher Jr., Appl. Phys. Lett. **81**, 5237 (2002).
[17] J. Zhao, J. P. Lu, J. Han, and C.-K. Yang, Appl. Phys. Lett. **82**, 3746 (2003).
[18] N. O. V. Plank, L. Jiang, and R. Cheung, Appl. Phys. Lett. **83**, 2426 (2003).
[19] J. D. Whittaker, M. Brink, G. A. Husseini, M. R. Linford, and R. C. Davis, Appl. Phys. Lett. **83**, 5307 (2003).
[20] S. Hofmann, C. Dukati, J. Robertson, and B. Kleinsorge, Appl. Phys. Lett. **83**, 135 (2003).
[21] E. I. Waldorff, A. M. Waas, P. P. Friedmann, and M. Keidar, J. Appl. Phys. **95**, 2749 (2004).
[22] I. Levchenko, M. Romanov, and M. Korobov, Surf. Coat. Technol. **184**, 356 (2004).
[23] V. Ligatchev, Rusli, and Z. Pan, Appl. Phys. Lett. **87**, 242903 (2005).
[24] M. Chhowalla, K. B. K. Teo, C. Ducati, N. L. Rupesinghe, G. A. J. Amaratunga, A. C. Ferrari, D. Roy, J. Robertson, and W. I. Milne, J. Appl. Phys. **90**, 5308 (2001).
[25] E. Tam, I. Levchenko, and K. Ostrikov, J. Appl. Phys. **100**, 036104 (2006).
[26] K. Ostrikov, Rev. Mod. Phys. **77**, 489 (2005).
[27] I. Levchenko, K. Ostrikov, M. Keidar, and S. Xu, Appl. Phys. Lett. **89**, 033109 (2006).